Title	Organization of Supramolecular Assemblies of Fullerene, Porphyrin and Fluorescein Dye Derivativeson on TiO_2 Nanoparticles for Light Energy Conversion
Author(s)	Hasobe, Taku; Hattori, Shigeki; Kamat, Prashant V.; Urano, Yasuteru; Umezawa, Naoki; Nagano, Tetsuo; Fukuzumi, Shunichi
Citation	Chemical Physics, 319(1-3): 243-252
Issue Date	2005-12-07
Type	Journal Article
Text version	author
URL	http://hdl.handle.net/10119/4951
Rights	NOTICE: This is the author's version of a work accepted for publication by Elsevier. Taku Hasobe, Shigeki Hattori, Prashant V. Kamat, Yasuteru Urano, Naoki Umezawa, Tetsuo Nagano and Shunichi Fukuzumi , Chemical Physics, 319(1-3), 2005, 243-252, http://dx.doi.org/10.1016/j.chemphys.2005.06.035
Description	

Organization of nanostructured supramolecular assembly of porphyrin and fluorescein dye derivatives with fullerene using TiO_2 nanoparticles for light energy conversion

Taku Hasobe,[a,b] Shigeki Hattori,[a] Prashant V. Kamat,[*,b] Yasuteru Urano,[c]
Naoki Umezawa,[c] Tetsuo Nagano,[*,c] and Shunichi Fukuzumi[*,a]

Department of Material and Life Science, Graduate School of Engineering, Osaka University, CREST, Japan Science and Technology Agency, Suita, Osaka 565-0871, Japan
Radiation Laboratory and Department of Chemical & Biomolecular Engineering, University of Notre Dame, Notre Dame, Indiana 46556, USA
Graduate School of Pharmaceutical Sciences, The University of Tokyo, Bunkyo-ku, Tokyo 113-0033, Japan

---

[a] Osaka University, [b] University of Notre Dame, [c] The University of Tokyo

Abstract

TiO_2 nanoparticles were modified with a porphyrin derivative, 5-[4-benzoic acid]-10,15,20-tris[3,5-di-*tert*-butylphenyl]-21*H*,23*H*-porphyrin (**H_2P-COOH**), and fluorescein derivatives, 9-[2-(3-carboxy-9,10-diphenyl)anthryl]-2,7-difluoro-6-hydroxy-3*H*-xanthen-3-one (**DPAX-COOH**) and 2',7'-difluorofluorescein (**FL-COOH**). The dye-modified TiO_2 nanoparticles were deposited on nanostructured OTE/SnO_2 electrode together with nanoclusters of fullerene (C_{60}) in acetonitrile/toluene (3:1, v/v) using an electrophoretic deposition technique to afford the dye-modified TiO_2 composite electrode denoted as OTE/SnO_2/(dye+C_{60})$_n$. The dye-modified TiO_2 composite electrodes have broad as well as high absorbance properties in the visible region, exhibiting the photoactive response under visible light excitation using I_3^-/I^- redox couple. The incident photon to photocurrent efficiency (IPCE) increases in order: OTE/SnO_2/(**H_2P**)$_n$ < OTE/SnO_2/(**H_2P-COO-TiO_2**)$_n$ < OTE/SnO_2/(**H_2P-COO-TiO_2**+C_{60}). The IPCE value is further improved when **H_2P-COOH** is replaced by a fluorescein derivative containing an electron donor moiety: **DPAX-COOH** (**DPA**: diphenylanthracene). The maximum IPCE value (42%) is obtained for OTE/SnO_2/(**DPAX-COO-TiO_2**+C_{60})$_n$ under the bias of 0.2 V vs SCE.

1. Introduction

In the past two decades, extensive endeavors have been devoted to develop molecular donor-acceptor systems (triads, tetrad, pentads, etc.), which can mimic a cascade of electron-transfer steps in the natural photosynthetic reaction center, leading to long-range charge separation with prolonged lifetime of the charge-separated state into second range [1-5]. In particular, fullerene holds a great promise as a spherical electron acceptor on account of the small reorganization energy in the electron transfer reactions [6,7]. Porphyrins on the other hand used as a photosensitizer are also suitable for efficient electron transfer with small reorganization energies. In addition, rich and extensive absorption features of porphyrinoid systems guarantees increased absorption cross-sections and an efficient use of the solar spectrum [8,9]. Thus, a combination of both chromophores (*i.e.*, porphyrins and fullerenes) seems ideal for fulfilling an enhanced light-harvesting efficiency of chromophores throughout the solar spectrum and a highly efficient conversion of the harvested light into the high energy state of the charge separation by photoinduced electron transfer [10,11]. Self-assembled monolayers (SAMs) of fullerenes and porphyrins have thereby merited special attention as artificial photosynthetic materials and photonic molecular devices [12-17]. However, such monolayer assemblies possess poor light-harvesting capability, affording low values of the incident photon-to-photocurrent efficiency (IPCE). In addition, the synthetic difficulty has precluded application of such artificial photosynthetic model compounds to develop low-cost photovoltaic devices [12-17].

In order to overcome these problems, we have previously reported a simple and new approach to prepare composite clusters of porphyrin and fullerene in a mixture of polar and nonpolar solvents, which are assembled as multilayers on a nanostructured SnO_2 electrode using an electrophoretic deposition technique [18]. The photoelectrochemical properties of the composite systems of porphyrin and fullerene are superior to those of the single component system [18]. In particular, multi-porphyrin arrays such as porphyrin dendrimers and porphyrin-modified gold nanoclusters with fullerenes exhibit much improved photoelectrochemical properties as compared with the composite clusters of monomeric porphyrin and fullerene [19,20]. However, the use of other dyes for composite nanoclusters with fullerene has yet to be explored.

On the other hand, fluorescein dyes have been widely employed to develop useful fluorescence probes for important biomolecules, such as nitric oxide and calcium ion, since fluorescence imaging is the most powerful technique currently available for continuous observation of the dynamic intracellular events of living cells [21-25]. The fluorescence quantum yields of fluorescein derivatives can be controlled by photoinduced electron transfer from the electron donor moiety to the singlet excited state of the xanthene moiety [24,25]. The occurrence of photoinduced charge separation has been demonstrated using a number of fluorescein-based probes in which electron donor moiety is directly linked with the xanthene moiety [25]. Fluorescein derivatives have also been used as suitable dyes to study interfacial electron transfer in organic photovoltaic devices [26-31]. The role of the dye molecule in light-energy conversion is not only to act as an antenna which captures the energy of sunlight, but also to initiate ultrafast electron injection from the singlet excited state of the dye into the conduction band of the semiconductor in the femtosecond time domain [26,27].

Assembly of dye-modified TiO_2 nanoparticles on electrodes using electrophoretic deposition technique has also been reported to be useful for preparation of organic thin films to obtain good electron acceptor materials [32-35]. The electrophoretic deposition of dye-modified TiO_2 nanoparticles on electrodes is an attractive method for preparation of organic multilayer films. However, assembly of the composite clusters of dye-modified TiO_2 nanoparticles and fullerene has yet to be examined.

We report herein a new type of organic solar cells based on composite nanoclusters of dye-modified TiO_2 nanoparticles and fullerene using two different type of dyes: porphyrin and fluorescein derivatives. The photoelectrochemical properties are changed depending on the type of dye molecules, 5-[4-benzoic acid]-10,15,20-tris[3,5-di-*tert*-butylphenyl]-21*H*,23*H*-porphyrin (**H_2P-COOH**), 9-[2-(3-carboxy-9,10-diphenyl)anthryl]-2,7-difluoro-6-hydroxy-3*H*-xanthen-3-one **(DPAX-COOH)**, and 2',7'-difluorofluorescein (**FL-COOH**), which are shown in Fig. 1. The porphyrin (**H_2P)** and fluorescein (**FL**) moieties are modified with carboxylic acid group (**H_2P-COOH, DPAX-COOH** and **FL-COOH** in Fig. 1) in order to be assembled on TiO_2 nanoparticles [denoted as **H_2P-COO-TiO_2**, **DPAX-COO-TiO_2** and **FL-COO-TiO_2** in Fig. 1, respectively]. The **DPAX** dye which contains an electron donor unit (**DPA**: diphenylanthracene) has been reported to afford a long lived charge-separated state upon photoexcitation of the xanthene moiety [25]. The dye-modified TiO_2 nanoparticles and fullerene nanoclusters are deposited as thin films on optically transparent electrode (OTE) of nanostructured SnO_2 (OTE/SnO_2) using an electrophoretic method as shown in Scheme 1. First, we examined the photoelectrochemical properties of composite cluster system using **H_2P-COOH** and fullerene (C_{60}) with TiO_2 nanoparticles on OTE/SnO_2 electrode [denoted as OTE/SnO_2/(**H_2P-COO-TiO_2**+C_{60})$_n$] relative to the reference system containing only **H_2P** (OTE/SnO_2/(**H_2P**)$_n$) and that without fullerene [OTE/SnO_2/(**H_2P-COO-TiO_2**)$_n$]. Then, we examined the photoelectrochemical properties of TiO_2 nanoparticles modified with **DPAX**

Fig. 1

[OTE/SnO_2/(**DPAX-COO-TiO_2**)$_n$] in comparison with those of a porphyrin derivative [OTE/SnO_2/(**H_2P-COO-TiO_2**)$_n$] and a fluorescein derivative without a donor unit [OTE/SnO_2/(**FL-COO-TiO_2**)$_n$]. Finally the best photoelectrochemical performance is achieved for nanostructured SnO_2 film of TiO_2 nanoparticles modified with composite clusters of **DPAX-COOH** and fullerene [denoted as OTE/SnO_2/(**DPAX-COO-TiO_2**+C_{60})$_n$], which is significantly superior to the single component films of an individual component as well as the reference systems without an electron donor unit (OTE/SnO_2/(**FL-COO-TiO_2**+C_{60})$_n$. Such a significant improvement of the multilayer system of composite TiO_2 nanoparticles with **DPAX** and C_{60} results from three-dimensional control of the molecular assembly and the efficient electron transfer in the supramolecular complex. The morphology and light energy conversion properties including the mechanism of these composite cluster systems are described in full detail in this paper.

Scheme 1

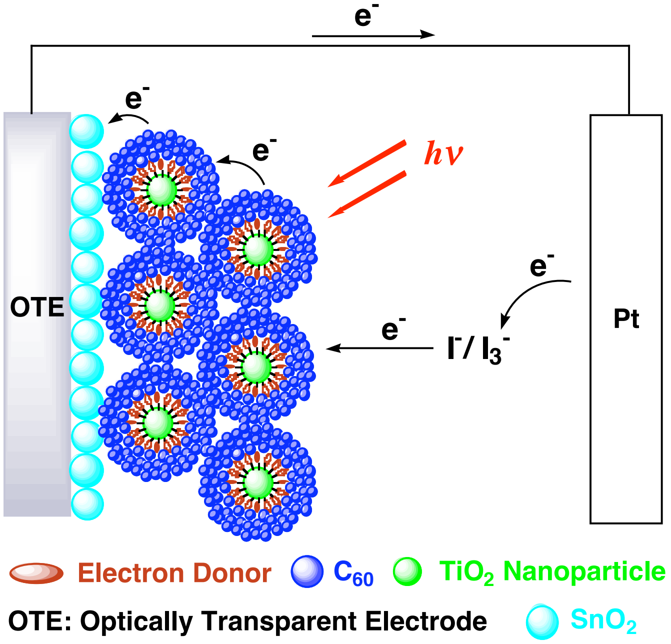

2. Experimental Section

2.1. General. Chemicals used in this study are of the best grade available, supplied by Tokyo Chemical Industries, Wako Pure Chemical, or Sigma Aldrich Co. ^{1}H NMR spectra were recorded on a JNM-AL300 (JEOL) instrument at 300 MHz. Matrix-assisted laser desorption/ionization (MALDI) time-of-flight (TOF) mass spectra were measured on a Kratos Compact MALDI I (Shimadzu). TiO_2 nanoparticles (P25, d = 21 nm) were purchased from Nippon Aerogel Co. Preparation of **H_2P**, **H_2P-COOH, DPAX-COOH** and **FL-COOH** has been described elsewhere [22].

2.2. Preparation of TiO_2 nanoparticles modified with dyes (H_2P-COO-TiO_2, DPAX-COO-TiO_2, and FL-COO-TiO_2). **H_2P-COOH, DPAX-COOH** and **FL-COOH** were prepared by immersing warmed TiO_2 nanoparticles (80 ~ 100 °C) in acetonitrile (10 mL) containing 3.0×10^{-4} mol dm^{-3} of **H_2P-COOH, DPAX-COOH**, and **FL-COOH** for 12 h, respectively. After adsorbing **H_2P-COOH, DPAX-COOH**, and **FL-COOH**, TiO_2 nanoparticles were filtered, and the subsequent washing with acetonitrile and drying afforded **H_2P-COO-TiO_2**, **DPAX-COO-TiO_2**, and **FL-COO-TiO_2**, respectively. The dye molecules were completely desorbed from TiO_2 particles into solution by immersing the dye-modified TiO_2 nanoparticles in methanol overnight. The amounts of **H_2P–COOH, DPAX–COOH**, and **FL–COOH** adsorbed on TiO_2 nanoparticles relative to the total weight were determined as 3.00×10^{-5}, 1.27×10^{-5}, and 1.73×10^{-5} mol/g, respectively.

2.3. Electrophoretic deposition of composite clusters on electrode. C_{60} is soluble in nonpolar solvents such as toluene. In mixed solvents (acetonitrile/toluene), however, they aggregate to form large size clusters with diameter of 100 nm - 300 nm [36,37]. The C_{60} cluster and TiO_2 nanoparticles were electrophoretically deposited onto SnO_2 films under an applied voltage as reported previously [32-37].

Nanostructured SnO_2 films were cast on an optically transparent electrode (OTE) by using a dilute (1-2%) colloidal solution (Alfa Chemicals), followed by annealing of the dried film at 673 K. Details about the electrode preparation and its properties have been described elsewhere [38]. These films are highly porous and electrochemically active to conduct charges across the film. The SnO_2 film electrode (OTE/SnO_2) and an OTE plate were introduced in a 1 cm path length cuvette and were connected to positive and negative terminals of the power supply, respectively. A known amount (~2 mL) of C_{60}, dye-modified TiO_2 nanoparticles (**H_2P-COO-TiO_2**, **DPAX-COO-TiO_2**, and **FL-COO-TiO_2**), or the mixed cluster suspension in acetonitrile/toluene (3/1, v/v) immediately after the ultrasonication was transferred to a 1 cm cuvette in which two electrodes (viz., OTE/SnO_2 and OTE) were kept at a distance of ~6 mm using a Teflon spacer. A dc voltage (500V) was applied between the two electrodes for 2 min using a Fluke 415 power supply. The deposition of the film can be visibly seen as the solution becomes colorless with simultaneous brown coloration of the SnO_2/OTE electrode. The SnO_2/OTE electrodes coated with dye-modified TiO_2 nanoparticles (**H_2P-COO-TiO_2**, **DPAX-COO-TiO_2**, and **FL-COO-TiO_2**) and C_{60} clusters are referred to OTE/SnO_2/(**H_2P-COO-TiO_2**+C_{60})$_n$, OTE/SnO_2/(**DPAX-COO-TiO_2**+C_{60})$_n$, and OTE/SnO_2/(**FL-COO-TiO_2**+C_{60})$_n$, respectively.

The UV-visible spectra were recorded on a Shimadzu 3101 spectrophotometer. Images were recorded using a Hitachi H600 transmission electron microscope. The morphology of the mesoporous electrodes was characterized by a scanning electron micrograph (SEM; JEOL, JSM-6700F).

2.4. Photoelectrochemical measurements. Photoelectrochemical measurements were performed using a standard three-compartment cell consisting of a working electrode and Pt wire gauze counter electrode and saturated calomel reference electrode (SCE). All photoelectrochemical measurements were performed in acetonitrile containing 0.5 mol dm^{-3}

NaI and 0.01 mol dm^{-3} I_2 with a Keithley model 617 programmable electrometer. A collimated light beam from a 150 W Xenon lamp with a 400 nm cut-off filter was used for excitation of the composite cluster films cast on SnO_2 electrodes. A Bausch and Lomb high intensity grating monochromator was introduced into the path of the excitation beam for selecting wavelength. A Princeton Applied Research (PAR) model 173 potentiostat and Model 175 universal programmer were used for recording I-V characteristics. The IPCE values were calculated by normalizing the photocurrent values for incident light energy and intensity using eqn. (1) [18],

$$\text{IPCE (\%)} = 100 \times 1240 \times I_{sc}/(W_{in} \times \lambda) \qquad (1)$$

where I_{sc} is the short circuit photocurrent (A/cm^2), W_{in} is the incident light intensity (W/cm^2), and λ is the wavelength (nm).

3. Results and discussion

3.1. Preparation and photoelectrochemical properties of the composite cluster film of H_2P-COO-TiO_2 and C_{60}. Porphyrin and C_{60} are soluble in nonpolar solvents such as toluene, but less so in polar solvents such as acetonitrile [18]. By the proper choice of polar to nonpolar solvent, we can achieve a controlled aggregation in the form of the composite nanoclusters. Detailed information of composite nanoclusters of porphyrin and C_{60} has been described elsewhere [18,36]. Upon subjecting the resultant cluster suspension to a high electric dc field (500 V for 2 min), porphyrin clusters [($\mathbf{H_2P}$)$_n$] were deposited onto an optically transparent electrode (OTE) of a nanostructured SnO_2 electrode (OTE/SnO_2), to afford the modified electrode. As the deposition continues we can visually observe discoloration of the solution and coloration of the electrode that is connected to positive terminal of the dc power supply. The absorption property of OTE/SnO_2/($\mathbf{H_2P}$)$_n$ ensures that incident light is absorbed strongly in the visible and near-infrared regions (spectrum a in Fig. 2A). On the other hand, TiO_2 nanoparticles were electrophoretically deposited onto the electrode in suspended solution [32-35]. The TiO_2 film modified with porphyrin (**$\mathbf{H_2P}$-COOH**) on OTE/SnO_2 electrode (OTE/SnO_2/(**$\mathbf{H_2P}$-COO-$\mathbf{TiO_2}$**)$_n$) is prepared in the same manner (dc voltage: 500 V for 2 min). A mixed cluster suspension of **$\mathbf{H_2P}$-COO-$\mathbf{TiO_2}$** and C_{60} was prepared in the total concentration range from 0.025 to 0.13 mmol dm^{-3} (molecular ratio of **$\mathbf{H_2P}$**:C_{60} = 1:5) in acetonitrile/toluene (3/1, v/v). Note that the mixed clusters were first prepared using different amounts of **$\mathbf{H_2P}$-COO-$\mathbf{TiO_2}$** and C_{60} to maintain their molar ratio as 1:5. The absorption property of OTE/SnO_2/(**$\mathbf{H_2P}$-COO-$\mathbf{TiO_2}$**)$_n$ is much higher than that of OTE/SnO_2/($\mathbf{H_2P}$)$_n$) (spectrum b in Fig. 2A). This indicates that the electrophoretic deposition of H_2P clusters with TiO_2 nanoparticles on OTE/SnO_2 electrode results in significant enhancement of light harvesting property [32-35]. In the case of OTE/SnO_2/(**$\mathbf{H_2P}$-COO-$\mathbf{TiO_2}$**+C_{60})$_n$, a broad absorption is observed in OTE/SnO_2/(**$\mathbf{H_2P}$-COO-$\mathbf{TiO_2}$**+C_{60})$_n$ in the visible region as compared with the reference system without C_{60} [OTE/SnO_2/(**$\mathbf{H_2P}$-COO-$\mathbf{TiO_2}$**)$_n$]. Such a broad absorption property of OTE/SnO_2/(**$\mathbf{H_2P}$-COO-$\mathbf{TiO_2}$**+C_{60})$_n$ may be ascribed to charge-transfer (CT) absorption between porphyrins and C_{60} [18,19].

Photoelectrochemical measurements were performed with a standard two-electrode system consisting of a working electrode and a Pt wire gauze electrode in 0.5 mol dm^{-3} NaI and 0.01 mol dm^{-3} I_2 in air-saturated acetonitrile. The maximum IPCE value of OTE/SnO_2/(**$\mathbf{H_2P}$-COO-$\mathbf{TiO_2}$**)$_n$ (~2%; spectrum a in Fig. 2B) is larger than that of OTE/SnO_2/($\mathbf{H_2P}$)$_n$ without TiO_2 (~1%; spectrum b in Fig. 2B). The IPCE value is further enhanced in OTE/SnO_2/(**$\mathbf{H_2P}$-COO-$\mathbf{TiO_2}$**+C_{60})$_n$ to reach ~6% (spectrum c in Fig. 2B).

Such an improvement of the IPCE value in OTE/SnO_2/(**H_2P-COO-TiO_2**+C_{60})$_n$ in comparison with the reference system demonstrates that molecular assembly of TiO_2 nanoparticles modified with porphyrin and C_{60} clusters play an important role in increasing the photocurrent generation as well as the light-harvesting efficiency.

Fig. 2

3.2. Composite cluster film of DPAX and C_{60} with TiO_2 nanoparticles.

We employed fluorescein derivatives instead of porphyrins in order to harvest light more widely in the visible region, since absorption region of fluorescein derivatives becomes red-shifted and broader as compared with porphyrin derivatives. In particular, **DPAX** containing an electron donor unit (**DPA**) has been reported to give the long lived charge-separated state upon photoexcitation of the xanthene moiety [25]. TiO_2 nanoparticles were modified with **DPAX** (**DPAX-COO-TiO_2**) and the reference materials without an electron donor unit (**FL-COO-TiO_2**). The OTE/SnO_2/(**DPAX-COO-TiO_2**)$_n$, OTE/SnO_2/(**DPAX-COO-TiO_2**+C_{60})$_n$, the reference systems [OTE/SnO_2/(**FL-COO-TiO_2**)$_n$ and OTE/SnO_2/(**FL-COO-TiO_2**+C_{60})$_n$] were prepared under the same conditions as employed for the porphyrin-modified TiO_2 electrodes (500 V for 2 min).

Strong and broad absorption of the OTE/SnO_2/(**DPAX-COO-TiO_2**+C_{60})$_n$ electrode in the visible region in Fig. 3a as compared with the absorption of **DPAX** in solution in Fig. 3b may be ascribed to intermolecular charge-transfer (CT) absorption between the donor moiety of **DPAX** and C_{60}, since such broad absorption is characteristic of an intermolecular CT band [39-41].

Fig. 3

3.3. Morphology of OTE/SnO_2/(DPAX+C_{60})$_n$. Scanning electron micrograph (SEM) was used to evaluate the morphology of the OTE/SnO_2/(**DPAX-COO-TiO_2**+C_{60})$_n$ film and the reference film [OTE/SnO_2/(C_{60})$_n$] as shown in Fig. 4. The OTE/SnO_2/(**DPAX-COO-TiO_2**+C_{60})$_n$ film is composed of closely packed clusters of about 20-100 nm size with a networked structure, which may result from a supramolecular interaction between **DPAX** and C_{60} on TiO_2 nanoparticles. In contrast with the OTE/SnO_2/(**DPAX-COO-TiO_2**+C_{60})$_n$ film, the OTE/SnO_2/(C_{60})$_n$ film without **DPAX**-modified TiO_2 nanoparticles contain a large size (100 – 300 nm) of nanoclusters [36,37].

Fig. 4

3.4. Photovoltage and photocurrent generation of OTE/SnO_2/(DPAX-COO-TiO_2+C_{60})$_n$ electrode. Photocurrent measurements were performed using the OTE/SnO_2/(**DPAX-COO-TiO_2**+C_{60})$_n$ electrode as a photoanode in acetonitrile containing 0.5 mol dm^{-3} NaI and 0.01 mol dm^{-3} I_2, which act as redox electrolyte, and a Pt gauge counter electrode [18.19]. The photovoltage and photocurrent responses recorded following the excitation of the OTE/SnO_2/(**DPAX-COO-TiO_2**+C_{60})$_n$ electrode at the visible light region (λ > 400 nm) are shown in Fig. 5A and 5B, respectively. The photocurrent response is prompt, steady, and reproducible during repeated on/off cycles of the visible light illumination. The short circuit photocurrent density (I_{sc}) is 0.13 mA/cm^2, and the open circuit voltage (V_{oc}) is 320 mV. Blank experiments conducted with OTE/SnO_2 (i.e., by excluding composite clusters (**DPAX-COO-TiO_2**+C_{60})$_n$ produced no detectable photocurrent under otherwise the same experimental conditions.

Fig. 5

A series of photocurrent action spectra were recorded in order to evaluate the photoresponse of the composite clusters towards the photocurrent generation. First, we compared with the photocurret action spectrum of OTE/SnO_2/(**DPAX-COO-TiO_2**)$_n$ with that of OTE/SnO_2/(**FL-COO-TiO_2**)$_n$ in which the dye contains no donor moiety in order to examine the effect of intramolecular charge separation on the IPCE values. The maximum IPCE value of OTE/SnO_2/(**DPAX-COO-TiO_2**)$_n$ (spectrum a in Fig. 6) is 23%, whereas that of OTE/SnO_2/(**FL-COO-TiO_2**)$_n$ (spectrum b in Fig. 6) is only 7.5%. This difference in the IPCE values results from the efficient charge separation in **DPAX** [25].

Fig. 6

We have also measured the photocurrent action spectra of OTE/SnO_2/(**DPAX-COO-TiO_2**+C_{60})$_n$ and OTE/SnO_2/(**FL-COO-TiO_2**+C_{60})$_n$ in order to evaluate the effect of C_{60} on the IPCE values. The IPCE value of OTE/SnO_2/(**DPAX-COO-TiO_2**+C_{60})$_n$ electrode reaches 33% (spectrum a in Fig. 7A), which is larger than the sum of two individual IPCE values (~26%) of OTE/SnO_2/(**DPAX-COO-TiO_2**)$_n$ and OTE/SnO_2/(C_{60})$_n$ with the same concentrations of **DPAX** and C_{60} (spectrum d in Fig. 7A). This indicates that the interaction between **DPAX** and C_{60} contributes to an increase in the IPCE value. The highest IPCE value of OTE/SnO_2/(**DPAX-COO-TiO_2**+C_{60})$_n$ is attained as 42% under the bias of 0.2 V vs. SCE, which is significantly larger than the corresponding value (13 %) of OTE/SnO_2/(**FL-COO-TiO_2**+C_{60})$_n$ as shown in Fig. 7B. Thus, the efficient photocurrent generation occurs in the supramolecular complex by modulating driving force of electron-transfer step (Fig. 7C) [18].

Fig. 7

2.6. Power conversion efficiency. We have also determined the power conversion efficiency (η) of the photoelectrochemical cell by varying the load resistance. The η value is calculated by eqn. (2) [18],

$$\eta = ff \text{ x } I_{sc} \text{ x } V_{oc}/\mathrm{W}_{in} \qquad (2)$$

where the fill factor (ff) is defined as $ff = P_{max}/(\mathrm{V}_{oc} \times I_{sc})$; P_{max} is the maximum power output of the cell, V_{oc} is the open circuit photovoltage, I_{sc} is the short circuit photocurrent. A decrease in the photovoltage accompanied by an increase in the photocurrent is observed with decreasing the load resistance as shown in Fig. 8. The detailed characteristics of the OTE/SnO_2/(**FL-COO-TiO_2**)$_n$, OTE/SnO_2/(**DPAX-COO-TiO_2**)$_n$, and OTE/-SnO_2/(**DPAX-COO-TiO_2+C_{60}**)$_n$ electrodes are summarized in Table 1. The I_{sc} and V_{oc} values of OTE/SnO_2/(**DPAX-COO-TiO_2**)$_n$ are much larger than those of OTE/SnO_2/(**FL-COO-TiO_2**)$_n$, which lead to 5 times improvement of the η value (0.24%) as compared with that of OTE/SnO_2/(**FL-COO-TiO_2**)$_n$ (0.050%). The η value is further enhanced by introducing C_{60} in OTE/SnO_2/(**DPAX-COO-TiO_2+C_{60}**)$_n$ (0.46%), which is about two times larger than that of OTE/SnO_2/(**DPAX-COO-TiO_2**)$_n$ (0.24%).

Fig. 8

3.7. Photocurrent generation mechanism. The photocurrent generation in the fluorescein-sensitized solar cells has previously been reported to be initiated by ultrafast electron injection from the singlet excited state of the fluorescein dye into the conduction band of the semiconductor in the femtosecond time domain [26,27]. In the case of the reference systems without C_{60} [**OTE/SnO_2/(FL-COO-TiO_2)$_n$**], the photoexcitation of the xanthene moiety results in electron injection from the singlet excited state of the dye into the conduction band and/or trap states of TiO_2 nanoparticles to produce the xanthene radical cation, since no electron donor moiety is linked with the xanthene moiety. The electrons collected on TiO_2 nanoparticles are furthermore injected into SnO_2 nanocrystallites ($E_{CB} = 0$ V *vs*. NHE) [18] to produce the photocurrent in the circuit. The resulting xanthene radical cation produced in the photoinduced electron injection to the conduction band of TiO_2 is reduced by electrolyte ($I_3^-/I^- = 0.5$ V vs. NHE) in the multilayer film [18,29]. At the counter electrode, the electron reduces the oxidized electrolyte (I_3^-), leading to the photocurrent generation.

On the other hand, the xanthene radical cation produced in the photoinduced electron injection from the singlet excited state of the xanthene dye to the conduction band of TiO_2 in OTE/SnO_2/(**DPAX-COO-TiO$_2$+C$_{60}$**)$_n$ may be efficiently reduced by the donor (DPA) moiety via efficient intramolecular electron transfer rather than electrolyte ($I_3^-/I^- = 0.5$ V vs NHE) via intermolecular electron transfer [18]. The resulting **DPA**$^{\bullet+}$ is reduced by electrolyte ($I_3^-/I^- = 0.5$ V vs NHE) to regenerate **DPA** [25]. Alternatively, the singlet excited state of the xanthene moiety is also quenched by electron transfer from the donor (**DPA**) moiety. The occurrence of such photoinduced electron transfer has been firmly established by the direct detection of the radical cation of the **DPA** moiety and the radical anion of the acceptor (xanthene) moiety in the laser flash photolysis experiments [25]. In such a case, the xanthene moiety can also act as an electron acceptor rather than an electron donor in contrast to the case of **FL** without a donor moiety. Since the xanthene moiety is located in close proximity of the semiconductor surface [31] and the redox potential of xanthene/xanthene$^{\bullet-}$ (-1.0 V vs NHE)[25] is lower than that of the conduction band of TiO_2 (-0.5 V vs NHE) [26,27], the resulting xanthene radical anion can inject an electron to the conduction band of TiO_2 nanoparticles. The electron is then injected from TiO_2 nanoparticles into SnO_2 nanocrystallites ($E_{CB} = 0$ V *vs*. NHE) [18] to produce the photocurrent in the circuit. In any case, DPA$^{\bullet+}$ is reduced by electrolyte (I_3^-/I^- = 0.5 V vs NHE) to regenerate DPA [18].

In the case of the composite cluster system (OTE/SnO$_2$/(**DPAX-COO-TiO$_2$**+C$_{60}$)$_n$, not only TiO$_2$ particles but also C$_{60}$ (C$_{60}$/C$_{60}^{\bullet-}$ = -0.2 V vs NHE) [18] act as an electron acceptor, leading to the enhancement of the photocurrent generation efficiency in OTE/SnO$_2$/(**DPAX-COO-TiO$_2$**+C$_{60}$) as compared with the system without C$_{60}$: OTE/SnO$_2$/(**DPAX-COO-TiO$_2$**)$_n$.

4. Conclusion

We have successfully constructed supramolecular photovoltaic cells composed of molecular nanocluster assemblies of fullerene and dyes such as porphyrin and xanthene derivatives, which are well organized with TiO$_2$ nanoparticles. The IPCE value of the composite cluster system of porphyrins and C$_{60}$ with TiO$_2$ nanoparticles (OTE/SnO$_2$/(**H$_2$P-COO-TiO$_2$**+C$_{60}$)$_n$) is improved as compared with the two reference systems [OTE/SnO$_2$/(**H$_2$P**)$_n$] and (OTE/SnO$_2$/(**H$_2$P-COO-TiO$_2$**)$_n$). The highest η value is achieved in OTE/SnO$_2$/(**DPAX-COO-TiO$_2$+C$_{60}$**)$_n$ (0.46%) composed of TiO$_2$ nanoparticles modified with a xanthene derivative (**DPAX**) containing the electron donor (**DPA**) moiety and C$_{60}$ clusters.

Acknowledgment

This work was partially supported by a Grant–in–Aid (No. 16205020) and by a COE program of Osaka University (Integrated Ecochemistry) from the Ministry of Education, Culture, Sports, Science, and Technology, Japan. PVK acknowledges the support from the Office of Basic Energy Science of the U. S. Department of the Energy. This is contribution No. NDRL XXXX from the Notre Dame Radiation Laboratory and from Osaka University.

We are grateful to Dr. Yuji Wada, Osaka University, for helping preparation of TiO_2 nanoparticles modified with dyes.

References and Notes

[1] D. Gust, T. A. Moore, A. L. Moore, in: V. Balzani (Ed.), Electron Transfer in Chemistry; Wiley-VCH, Weinheim, 2001, vol. 3, pp 27.

[2] K. D. Jordan, M. N. Paddon-Row, Chem. Rev. 92 (1992) 395.

[3] A. Harriman, J.-P. Sauvage, Chem. Soc. Rev. 25 (1996) 41.

[4] M. R. Wasielewski, Chem. Rev. 92 (1992) 435.

[5] D. Gust, T. A. Moore, A. L. Moore, Acc. Chem. Res. 34 (2001) 40.

[6] S. Fukuzumi, H. Imahori, in: V. Balzani, (Ed.) Electron Transfer in Chemistry, Wiley-VCH, Weinheim, 2001, Vol. 2, pp 927.

[7] S. Fukuzumi, D. M. Guldi, in: Balzani, V. (Ed.) Electron Transfer in Chemistry, Wiley-VCH, Weinheim, 2001, Vol. 2, pp 270.

[8] S. Fukuzumi, in: K. M. Kadish, K. M. Smith, R. Guilard, (Eds.) The Porphyrin Handbook, Academic Press, San Diego, 2000, Vol. 8, pp 115.

[9] S. Fukuzumi, Y. Endo, H. Imahori, J. Am. Chem. Soc. 124 (2002) 10974.

[10] S. Fukuzumi, Pure Appl. Chem. 75 (2003) 577.

[11] S. Fukuzumi, Org. Biomol. Chem. 1 (2003) 609.

[12] L. Echegoyen, L. E. Echegoyen, Acc. Chem. Res. 31 (1998) 593.

[13] D. Hirayama, K. Takimiya, Y. Aso, T. Otsubo, T. Hasobe, H. Yamada, H. Imahori, S. Fukuzumi, Y. Sakata, J. Am. Chem. Soc. 124 (2002) 532.

[14] M. Lahav, V. Heleg-Shabtai, J. Wasserman, E. Katz, I. Willner, H. Dürr, Y.-Z. Hu, S. H. Bossmann, J. Am. Chem. Soc. 122 (2000) 11480.

[15] K. Uosaki, T. Kondo, X.-Q. Zhang, M. Yanagida, J. Am. Chem. Soc. 119 (1997) 8367.

[16] I. Willner, V. Heleg-Shabtai, E. Katz, H. K. Rau, W. Haehnel, J. Am. Chem. Soc. 121 (1999) 6455.

[17] H. Imahori, H. Norieda, H. Yamada, Y. Nishimura, I. Yamazaki, Y. Sakata, S. Fukuzumi, J. Am. Chem. Soc. 123 (2001) 100.

[18] T. Hasobe, H. Imahori, S. Fukuzumi, P. V. Kamat, J. Phys. Chem. B 107 (2003) 12105.

[19] T. Hasobe, P. V. Kamat, M. A. Absalom, Y. Kashiwagi, J. Sly, M. J. Crossley, K. Hosomizu, H. Imahori, S. Fukuzumi, J. Phys. Chem. B 108 (2004) 12865.

[20] T. Hasobe, H. Imahori, P. V. Kamat, S. Fukuzumi, J. Am. Chem. Soc. 125 (2003) 14962.

[21] A. Minta, J. P. Y. Kao, R. Y. Tsien, J. Biol. Chem. 264 (1989) 8171.

[22] N. Umezawa, K. Tanaka, Y. Urano, K. Kikuchi, T. Higuchi, T. Nagano, Angew. Chem., Int. Ed. 38 (1999) 2899.

[23] G. K. Walkup, S. C. Burdette, S. J. Lippard, R. Y. Tsien, J. Am. Chem. Soc. 2000 (122) 5644.

[24] K. Tanaka, T. Miura, N. Umezawa, Y. Urano, K. Kikuchi, T. Higuchi, T. Nagano, J. Am. Chem. Soc. 123 (2001) 2530.

[25] T. Miura, Y. Urano, K. Tanaka, T. Nagano, K. Ohkubo, S. Fukuzumi, J. Am. Chem. Soc. 125 (2003) 8666.

[26] S. Pelet, M. Grätzel, J.-E. Moser, J. Phys. Chem. B 107 (2003) 3215.

[27] G. Benkö, B. Skårman, R. Wallenberg, A. Hagfeldt, V. Sundström, P. A. Yartsev, J. Phys. Chem. B 107 (2003) 1370.

[28] A. Hagfeldt, M. Grätzel, Chem. Rev. 95 (1995) 49.

[29] A. Hagfeldt, M. Grätzel, Acc. Chem. Res. 33 (2000) 269.

[30] G. Benkö, M. Hilgendorff, A. P. Yartsev, V. Sundström, J. Phys. Chem. B 105 (2001) 967.

[31] S. Hattori, T. Hasobe, K. Ohkubo, Y. Urano, N. Umezawa, T. Nagano, Y. Wada, S. Yanagida, S. Fukuzumi, J. Phys. Chem. B 108 (2004) 15200.

[32] Y. Matsumoto, M. Noguchi, T. Matsunaga, K. Kamada, M. Koinuma, S. Yamada, Electrochemistry 69 (2001) 314.

[33] T. Miyasaka, Y. Kijitori, T. N. Murakami, M. Kimura, S. Uegusa, Chem. Lett. 2002, 1250.

[34] D. Matthews, A. Kay, M. Grätzel, Aust. J. Chem. 47 (1994) 1869.

[35] D. Xu, Y. Xu, D. Chen, G. Guo, L. Gui, Y. Tang, Adv. Mater. 12 (2000) 520.

[36] S. Barazzouk, S. Hotchandani, P. V. Kamat, Adv. Mater. 13 (2001) 1614.

[37] P. V. Kamat, S. Barazzouk, K. G. Thomas, S. Hotchandani, J. Phys. Chem. B 104 (2000) 4014.

[38] I. Bedja, S. Hotchandani, P. V. Kamat, J. Phys. Chem. 98 (1994) 4133.

[39] Fukuzumi, K. Ohkubo, Y. Tokuda, T. Suenobu, J. Am. Chem. Soc. 122 (2000) 4286.

[40] R. S. Mulliken, W. B. Person, Molecular Complexes. A Lecture and Reprint Volume, York, 1969.

[41] R. Foster, Organic Charge-Transfer Complexes, Academic Press, New York, 1969.

Table 1. Performance Characteristics of OTE/SnO_2/(**FL-COO-TiO_2**)$_n$, OTE/SnO_2-/(**DPAX-COO-TiO_2**)$_n$, and OTE/SnO_2/(**DPAX-COO-TiO_2**+C_{60})$_n$

System	V_{oc} (mV)	I_{sc} (mA cm^{-2})	*ff*	η (%)^a
(FL-COO-TiO_2)$_n$	160	0.034	0.31	0.050
(DPAX-COO-TiO_2)$_n$	280	0.093	0.31	0.31
(DPAX-COO-TiO_2+C_{60})$_n$	320	0.13	0.38	0.38

^{a} electrolyte: 0.5 mol dm^{-3} NaI and 0.01 mol dm^{-3} I_2 in acetonitrile; white light illumination ($\lambda > 400$ nm); input power; 3.4 mW cm^{-2}.

Figure Captions

Fig. 1. TiO_2 nanoparticles modified with dyes and the reference compounds employed in this study.

Fig. 2. (A) Absorption spectra of (a) OTE/SnO_2/($\mathbf{H_2P}$)$_n$ ([$\mathbf{H_2P}$] = 0.19 mmol dm^{-3}), (b) OTE/SnO_2/($\mathbf{H_2P\text{-}COO\text{-}TiO_2}$)$_n$ ([$\mathbf{H_2P}$] = 0.025 mmol dm^{-3}), (c) OTE/SnO_2/($\mathbf{H_2P\text{-}COO\text{-}TiO_2}$+$C_{60}$)$_n$ ([$\mathbf{H_2P}$] = 0.025 mmol dm^{-3}, [C_{60}] = 0.13 mmol dm^{-3}), and (d) $\mathbf{H_2P\text{-}COOH}$ in toluene (10 μmol dm^{-3}). (B) Photocurrent action spectra (IPCE vs wavelength) of OTE/SnO_2/($\mathbf{H_2P}$+C_{60})$_n$ ([$\mathbf{H_2P}$] = 0.19 mmol dm^{-3}), (b) (OTE/SnO_2/($\mathbf{H_2P\text{-}COO\text{-}TiO_2}$)$_n$ ([$\mathbf{H_2P}$] = 0.025 mmol dm^{-3}), and (c) OTE/SnO_2/($\mathbf{H_2P\text{-}COO\text{-}TiO_2}$+$C_{60}$)$_n$ ([$\mathbf{H_2P}$] = 0.025 mmol dm^{-3}; [C_{60}] = 0.13 mmol dm^{-3}); electrolyte: 0.5 mol dm^{-3} NaI and 0.01 mol dm^{-3} I_2 in acetonitrile.

Fig. 3. Absorption spectra of (a) OTE/SnO_2/($\mathbf{DPAX\text{-}COO\text{-}TiO_2}$+$C_{60}$)$_n$ ([**DPAX**] = 0.025 mmol dm^{-3}, [C_{60}] = 0.13 mmol dm^{-3}) and (b) $\mathbf{DPAX\text{-}COO\text{-}TiO_2}$ in 0.1 mol dm^{-3} NaOH aq. solution (pH 13) ([**DPAX**] = 10 μmol dm^{-3}).

Fig. 4. SEM (scanning electron micrograph) images of (A) OTE/SnO_2/($\mathbf{DPAX\text{-}COO\text{-}TiO_2}$+$C_{60}$)$_n$ ([**DPAX**] = 0.025 mmol dm^{-3}, [C_{60}] = 0.13 mmol dm^{-3}) and (B) OTE/SnO_2/(C_{60})$_n$ ([C_{60}] = 0.13 mmol dm^{-3}).

Fig. 5. (A) Photovoltage and (B) photocurrent generation at OTE/SnO_2/($\mathbf{DPAX\text{-}COO\text{-}TiO_2}$+$C_{60}$)$_n$ ([**DPAX**] = 0.025 mmol dm^{-3}, [C_{60}] = 0.13 mmol dm^{-3}) under illumination of white light ($\lambda > 400$ nm); electrolyte: 0.5 mol dm^{-3} NaI and 0.01 mol dm^{-3} I_2 in acetonitrile; input power: 3.4 mW cm^{-2}.

Fig. 6. Photocurrent action spectra of (a) OTE/SnO_2/(**DPAX-COO-TiO_2**)$_n$ ([**DPAX**] = 0.025 mmol dm^{-3}) and (b) OTE/SnO_2/(**FL-COO-TiO_2**)$_n$ ([**FL**] = 0.025 mmol dm^{-3}) with no applied bias potential.

Fig. 7. (A) Photocurrent action spectra of (a) OTE/SnO_2/(**DPAX-COO-TiO_2+C_{60}**)$_n$ ([**DPAX**] = 0.025 mmol dm^{-3}; [C_{60}] = 0.13 mmol dm^{-3}) with no applied bias potential, (b) OTE/SnO_2/(**DPAX-COO-TiO_2**)$_n$ ([**DPAX**] = 0.025 mmol dm^{-3}) with no applied bias potential, (c) OTE/SnO_2/(C_{60})$_n$ ([C_{60}] = 0.13 mmol dm^{-3}) with no applied bias potential, and (d) the sum of the IPCE response of (b) OTE/SnO_2/(**DPAX-COO-TiO_2**+C_{60})$_n$ and (c) OTE/SnO_2/(C_{60})$_n$. (B) Photocurrent action spectra (IPCE *vs.* wavelength) of (a) OTE/SnO_2/(**DPAX-COO-TiO_2**+C_{60})$_n$ ([**DPAX**] = 0.025 mmol dm^{-3}; [C_{60}] = 0.13 mmol dm^{-3}) at an applied bias potential of 0.2 V *vs.* SCE and (b) OTE/SnO_2/(**FL-COO-TiO_2**+C_{60})$_n$ ([**FL**] = 0.025 mmol dm^{-3}; [C_{60}] = 0.13 mmol dm^{-3} at an applied bias potential of 0.2 V *vs.* SCE. (C) I-V characteristic of the OTE/SnO_2/(**DPAX-COO-TiO_2**+C_{60})$_n$ ([**DPAX**] = 0.025 mmol dm^{-3}, [C_{60}] = 0.13 mmol dm^{-3}) under illumination of white light (λ > 400 nm); electrolyte: 0.5 mol dm^{-3} and NaI and 0.01 mol dm^{-3} and I_2 in acetonitrile; input power: 3.4 mW cm^{-2}.

Fig. 8. Power characteristic of (a) OTE/SnO_2/(**DPAX-COO-TiO_2**+C_{60})$_n$ ([**DPAX**] = 0.025 mmol dm^{-3}, [C_{60}] = 0.13 mmol dm^{-3}), (b) OTE/SnO_2/(**DPAX-COO-TiO_2**)$_n$ ([**DPAX**] = 0.025 mmol dm^{-3}), and (c) OTE/SnO_2/(**FL-COO-TiO_2**)$_n$ ([**FL**] = 0.025 mmol dm^{-3}) under white light illumination (λ> 400 nm); electrolyte: 0.5 mol dm^{-3} NaI and 0.01 mol dm^{-3} I_2 in acetonitrile; input power: 3.4 mW cm^{-2}.

Fig. 1

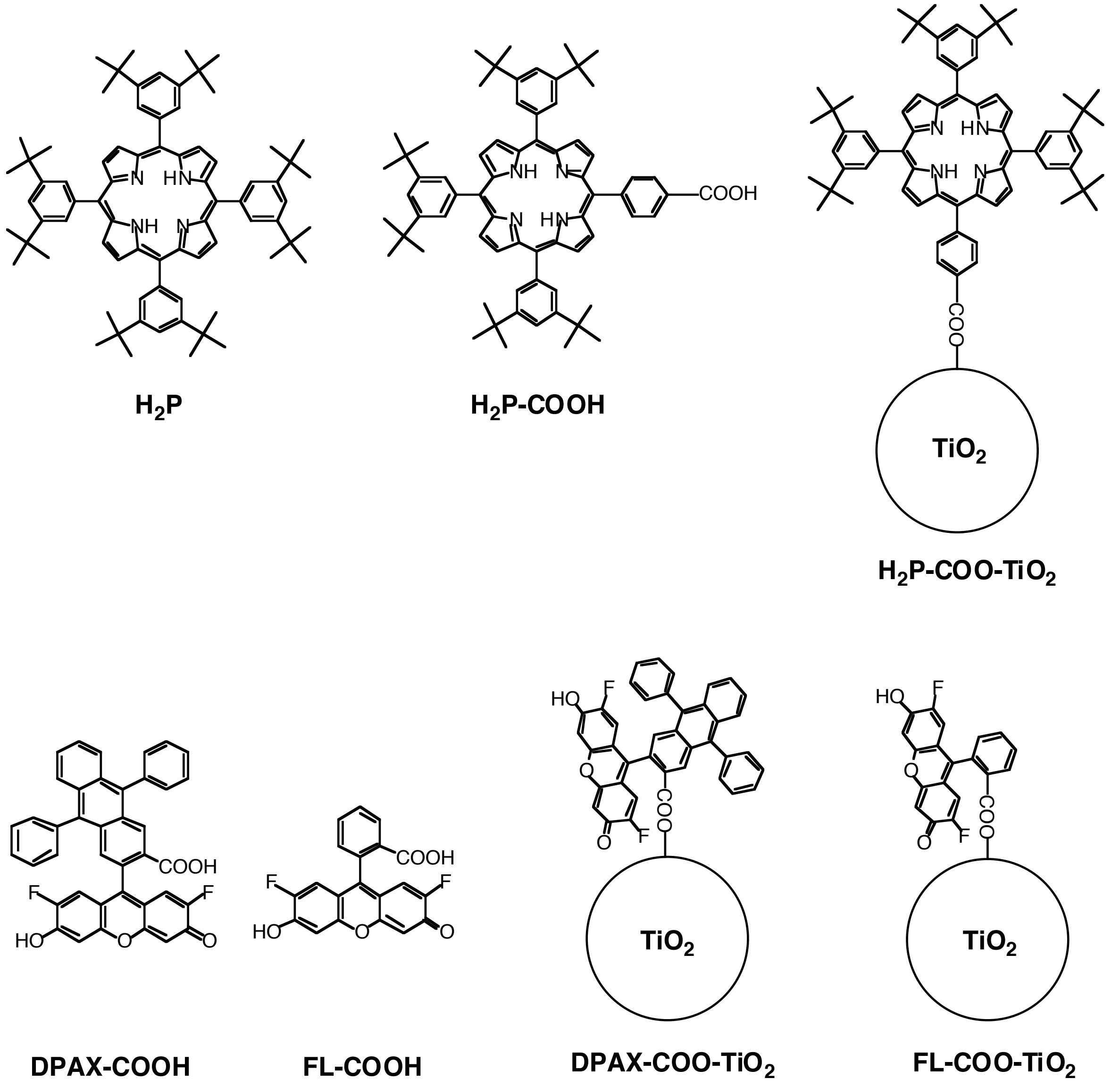
H2P
H2P-COOH
H2P-COO-TiO2
DPAX-COOH
FL-COOH
DPAX-COO-TiO2
FL-COO-TiO2
COOH
TiO2
N
NH
HN
HO
F
O

Fig. 2

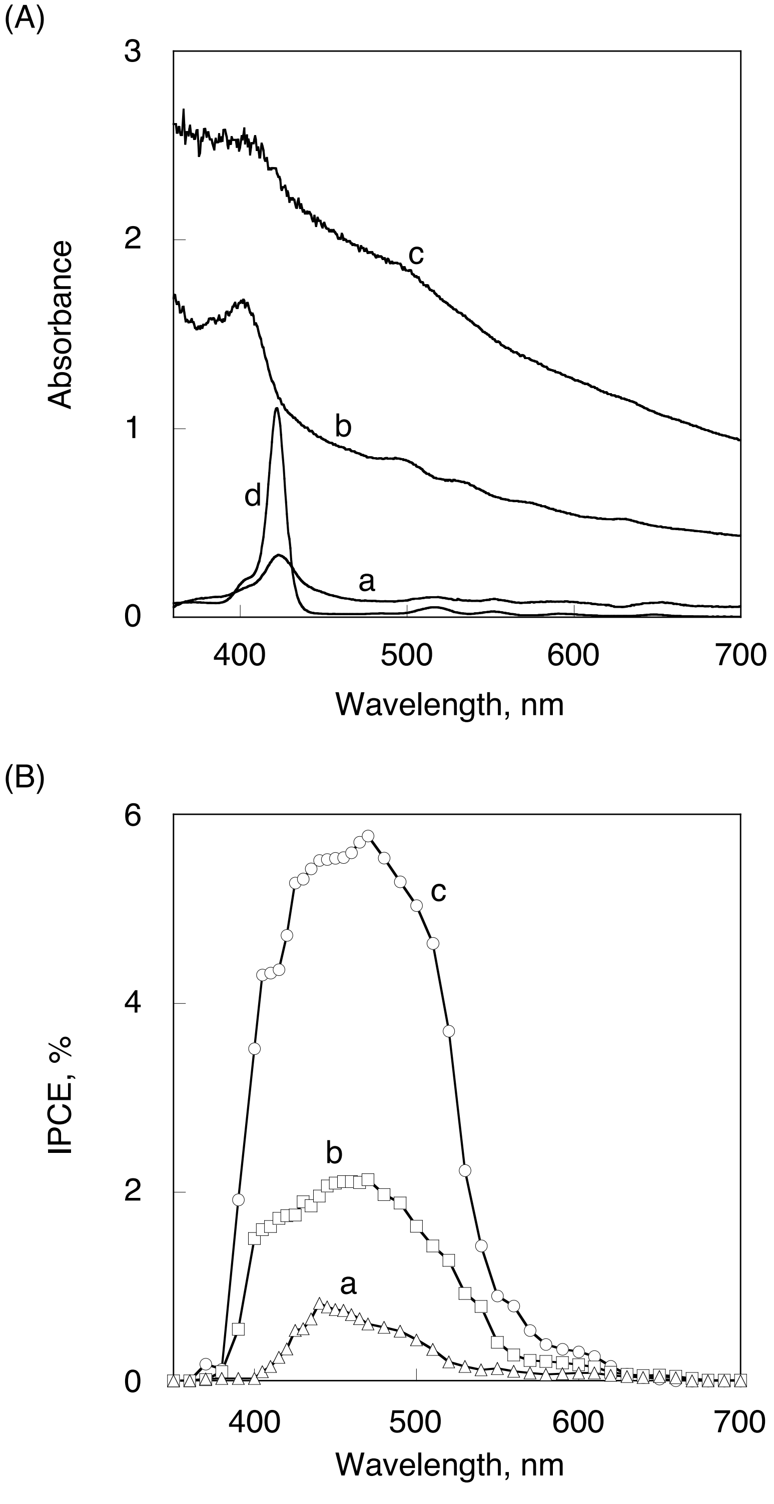

(A)
Absorbance
3
2
1
0
c
b
d
a
400
500
600
700
Wavelength, nm
(B)
IPCE, %
6
4
2
0
c
b
a
400
500
600
700
Wavelength, nm

Fig. 3

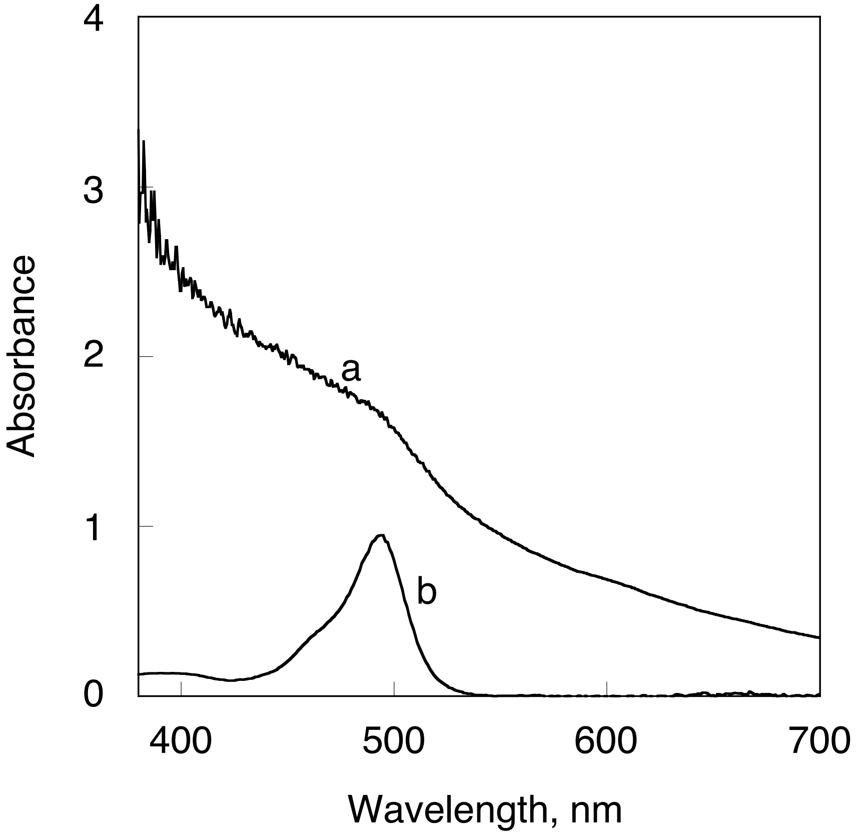

Fig. 4

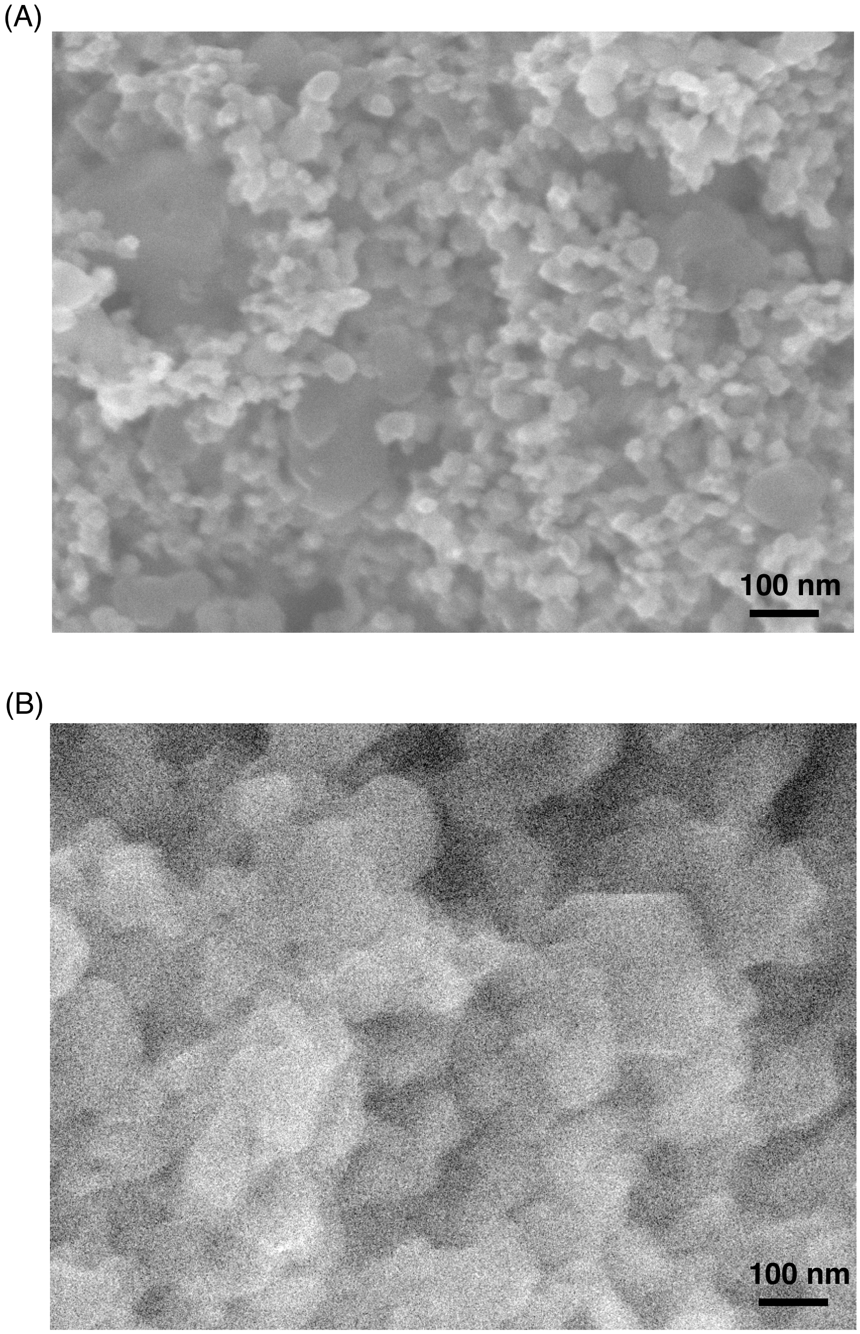

Fig. 5

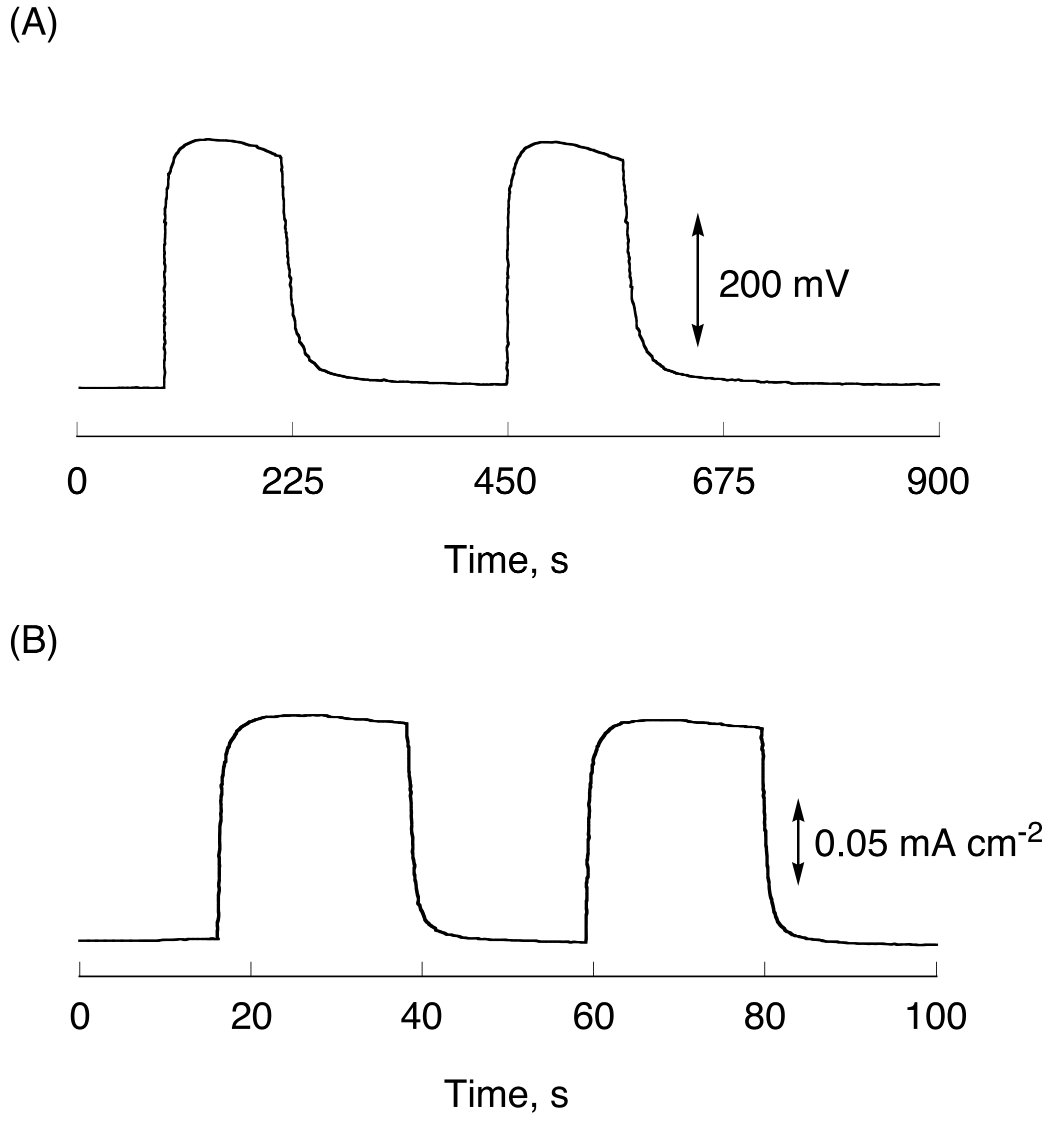
(A)
200 mV
0
225
450
675
900
Time, s
(B)
0.05 mA cm^{-2}
0
20
40
60
80
100
Time, s

Fig. 6

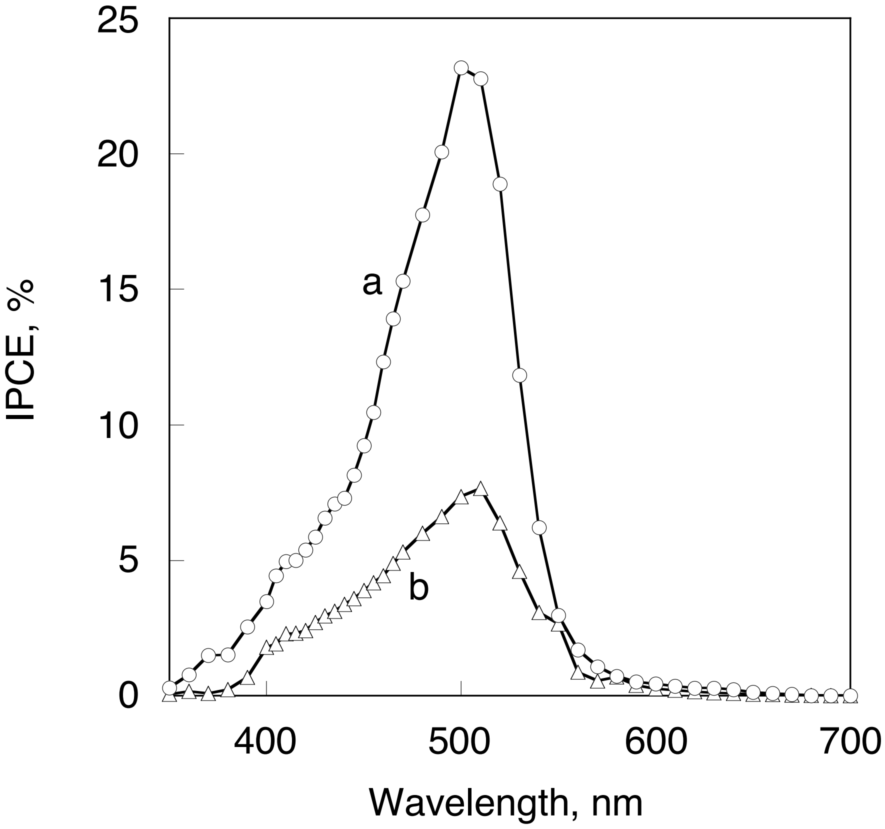

Fig. 7

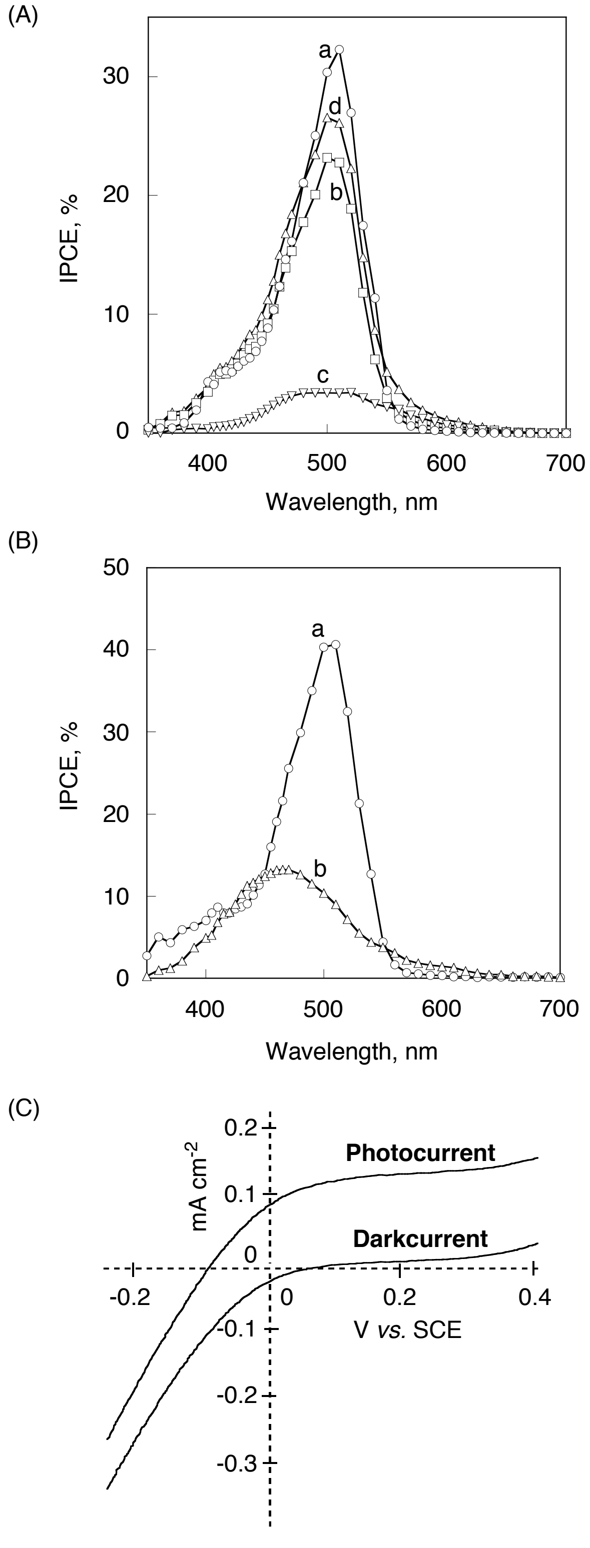
(A)
IPCE, %
0
10
20
30
400
500
600
700
Wavelength, nm
a
d
b
c
(B)
IPCE, %
0
10
20
30
40
50
400
500
600
700
Wavelength, nm
a
b
(C)
mA cm-2
0.2
0.1
0
-0.1
-0.2
-0.3
-0.2
0
0.2
0.4
V vs. SCE
Photocurrent
Darkcurrent

Fig. 8

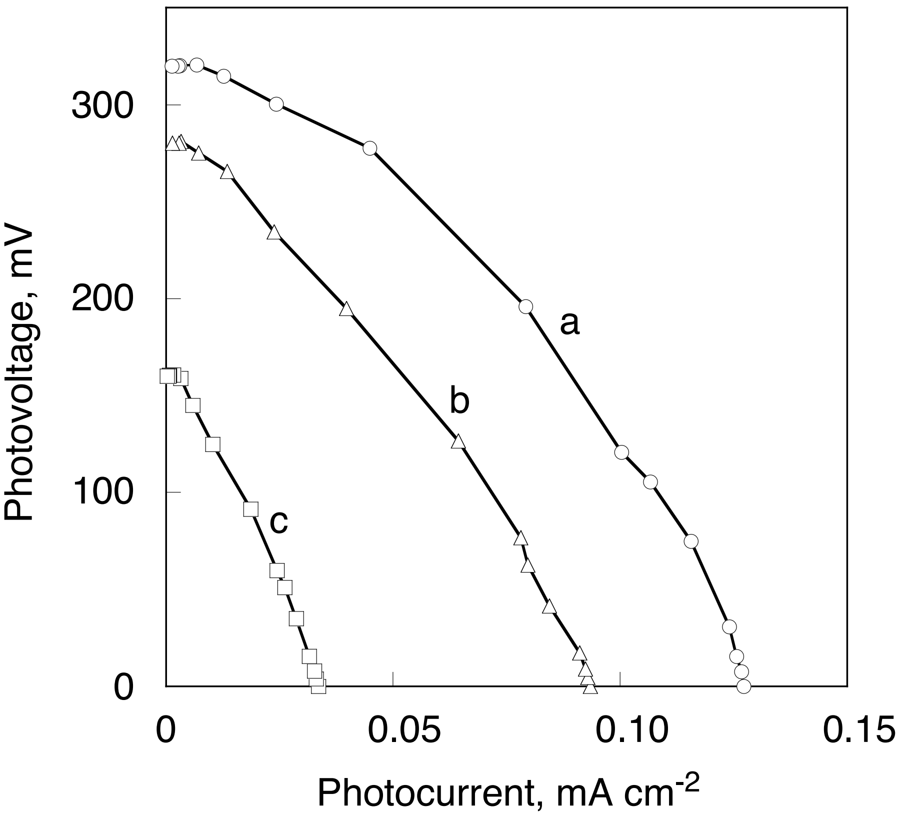

Photovoltage, mV
0
100
200
300
0
0.05
0.10
0.15
Photocurrent, mA cm-2
a
b
c